

# A Predictive Switching Modulator for Current Mode Control of High Power Factor Boost Rectifier

S. Chattopadhyay, V. Ramanarayanan and V. Jayashankar

Department of Electrical Engineering,

Indian Institute of Science, Bangalore 560012, India

**Abstract** - In this paper, a new variation of current mode control for high power factor Boost rectifier is presented. The general features are - no input voltage sensing, no use of multiplier, and no inner current regulator. It therefore follows the same control structure as that of Linear Peak Current Mode Control (LPCM) and Non Linear Carrier Control (NLC). However it implements a different equation for the modulator that extends the range of continuous conduction mode (CCM) of operation. The controller is predictive as the actual current equals the reference current at the end of each switch period.

## I. INTRODUCTION

A diode bridge rectifier followed by a Boost converter most often constitutes the power circuit of single phase Power Factor Correction (PFC) rectifier. The controller of PFC should shape the input current ( $i_g$ ) to follow the same waveshape as the input voltage ( $v_g$ ). Using this definition of control objective remarkable simplification in the control structure of PFC rectifier has been achieved by controllers such as Nonlinear Carrier Control (NLC) [2], [4] and Linear Peak Current Mode Control (LPCM) [1]. The Boost rectifier power circuit and the general controller structure of NLC and LPCM are shown in Fig.1.

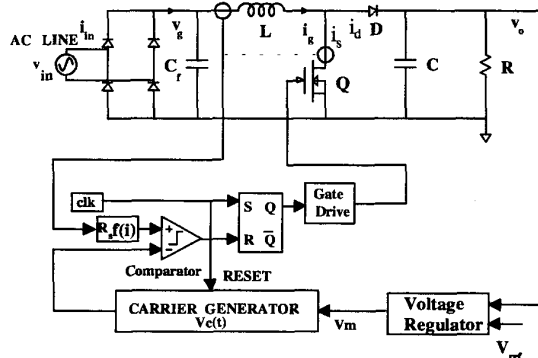
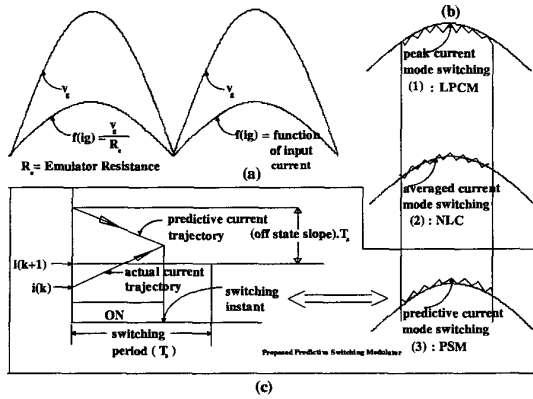


Fig. 1. Power Circuit of single phase PFC Boost rectifier along with general control structure of Nonlinear Carrier Control (NLC), Linear Peak Current Mode Control (LPCM) and Predictive Switching Modulator (PSM) that is proposed here

In these controllers the inner loop current regulator is eliminated and input voltage sensing is not required. The analog multiplier is not present as the dc reference does not have to be converted into sinusoidal reference. The resulting modulator determines the duty ratio by solving periodically an equation, one side of which is a certain function of the sensed current (for example average of the switch current for NLC) and the other side is the carrier waveform derived after processing the voltage regulator output. The difference between NLC and LPCM is this : through the generation of an appropriate carrier, the NLC controller implements average current mode control whereas LPCM would generate a different carrier waveform to implement the objective of peak current mode control.

In this paper a Predictive Switching Modulator (PSM) for Current Mode control of PFC Boost rectifier is proposed. The defining equation of this strategy equates the estimated inductor current at the end of the switching period ( $T_s$ ) with the reference current to determine the duty ratio. The estimation is possible since the input voltage is practically constant over a switching period. This enables us to predict the current ripple of the subsequent OFF period during the ON time itself. The ripple current expressed as a function of time valid between ( $0 < t \leq T_s$ ) can be algebraically added with the ON state current to determine the inductor current at the end of the switching period. The advantage of PSM is the extended region of CCM operation of the Boost rectifier. The disadvantages of DCM operation in the form of distortion in the current waveform is well known. The Predictive Switching Modulator (PSM) is well suited for analysis. The modulator can be configured as a standard Current Programmed Controller with a nonlinear compensating waveform. Therefore following the same procedure as in [3] steady state stability limit can be derived and a low frequency small signal model of the rectifier can be obtained.

In section II the configuration of the proposed modulator - Predictive Switching Modulator (PSM) is described. Section III gives the steady state stability analysis of the PSM. Section IV defines the range of CCM. In section V, the procedure for the derivation of small signal model is presented.



**Fig. 2. (a) Generalized control objective of current mode control of Boost rectifier**  
**(b) Specific control objectives of different types of current mode control**  
**(c) Operating principle of Predictive Switching Modulator (PSM)**

## 11. PREDICTIVE SWITCHING MODULATOR (PSM)

The generalized control objective of a high power factor Boost rectifier can be expressed as

$$f(i_g) = \frac{v_g}{R_e} \quad 0 < t \leq T_s \quad (1)$$

where  $R_e$  is the emulated resistance. For NLC equation (2) and for LPCM equation (3) are specific expressions of  $f(i_g)$ .

$$f(i_g) = \frac{1}{T_s} \int_0^{T_s} i_g dt \quad (2)$$

$$f(i_g) = i_g[dT_s] \quad (3)$$

For PSM that has been proposed here equation (4) will be satisfied.

$$f(i_g) = i_g[T_s] \quad (4)$$

Fig.2(a) shows the same idea. Fig.2(b) illustrates the difference between the control objectives of (1) LPCM, (2) NLC and (3) PSM. Fig.2(c) shows how the switching instant is determined in PSM. For a Boost rectifier the switch current is equal to the input current during ON time of the switch and from protection point of view switch current sensing is preferred over input current sensing. Therefore the modulators of NLC, LPCM and PSM will implement (5),(6) and (7) respectively instead of (2),(3) and (4).

$$\frac{1}{T_s} \int_0^{dT_s} i_s dt = di_{gav} = d \frac{v_g}{R_e} \quad (5)$$

$$i_s[dT_s] = \frac{v_g}{R_e} \quad (6)$$

$$i_s[T_s] = \frac{v_g}{R_e} \quad (7)$$

The right hand side of (5), (6) is expressed by a suitable carrier waveform [1],[2]. We need to generate a carrier for PSM also that would satisfy (7). The function of a modulator is to determine the time at which two time varying signals become equal in a defined switching period. For the PSM the generation of the carrier can be explained as follows : in the  $k$  th period when the converter is operating in CCM, the OFF state topology of the converter is known during ON time itself. Since the input and output voltages are slow varying compared to the switching frequency ( $F_s$ ), the OFF state slope of the current can be predicted. so a predictive trajectory of the OFF state current can be generated through extrapolation. Now by adding this ripple current with the desired final current  $i(k+1)$ , which is available as reference, the complete predictive current trajectory can be obtained. The switching occurs when the actual current crosses the predictive current trajectory. In each switching period, the equation of the predictive current, which is the carrier waveform  $i_c(t)$ , can be expressed as

$$i_c(t) = \frac{v_g}{R_e} + \frac{v_{off} T_s}{L} (1 - \frac{t}{T_s}) \quad (8)$$

where  $v_{off}$ , is the OFF state voltage across the Boost inductor ( $L$ ). In actual implementation,  $v_g$  is not sensed, instead (11) is used, which can be derived using (9) and (10).

$$v_g = v_o (1 - \frac{t}{T_s}) \quad (9)$$

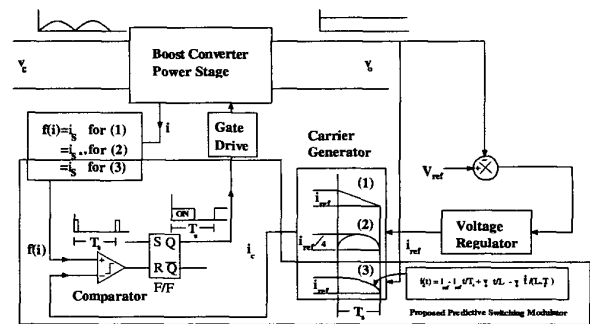


**Fig. 3. Block Diagram of (1) : LPCM**  
**(2) : NLC**  
**(3) : PSM**

$$i_{ref} = \frac{v_o}{R_e} \quad (10)$$

$$i_c(t) = i_{ref}(1 - \frac{t}{T_s}) + \frac{v_o T_s}{L} \frac{t}{T_s} (1 - \frac{t}{T_s}) \quad (11)$$

Fig.3 shows the block diagram of the proposed PSM along with LPCM and NLC methods of current control.

### III. STEADY STATE STABILITY

Current mode control may exhibit steady state stability problem under certain operating conditions because of the presence of a local feedback in its control structure [3]. In this section we carry out the stability analysis of the PSM. The method followed here is a graphical one and basically the same as in [3] with necessary modifications made for a nonlinear compensating waveform. The carrier  $i_c(t)$  is configured in the standard structure of (12), shown in Fig. 4(a).

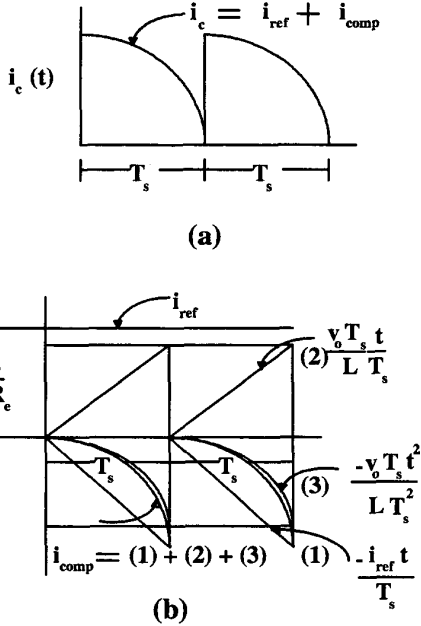


Fig. 4. (a) Carrier waveform ( $i_c$ ) of PSM  
(b) Reference ( $i_{ref}$ ) and different components of the Compensating waveform ( $i_{comp}$ )

$$i_c(t) = i_{ref} + i_{comp}(t) \quad (12)$$

where

$$i_{comp}(t) = -i_{ref} \frac{t}{T_s} + \frac{v_o T_s}{L} \frac{t}{T_s} - \frac{v_o T_s}{L} \quad (13)$$

The compensating waveform consists of components of linear and non-linear ramps, as shown in Fig.4(b).

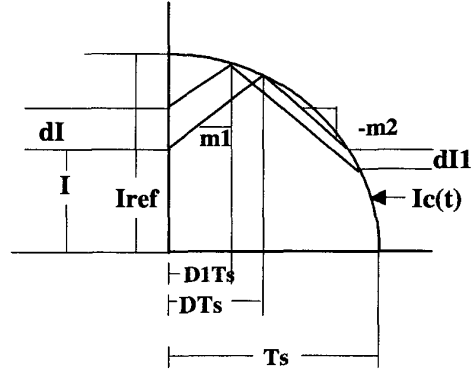


Fig.5. Current Mode Control with nonlinear ramp  
Initial perturbation of  $\delta I$  gets propagated as  $\delta I1$  in the next cycle.  $I_c(t)$  is the carrier waveform of PSM.

In this analysis we will give an initial perturbation  $\delta I$  to the steady inductor current and then will find out the amount  $\delta I1$  by which this perturbation will propagate at the end of the switching cycle. This is shown graphically in Fig. 5. But first we need to rewrite the equation of the carrier  $I_c(t)$  in terms of coefficients of first order ( $m_x$ ) and second order ( $m_y$ ) compensating ramps .

$$I_c(t) = I_{ref} - m_x T_s \frac{t}{T_s} - m_y T_s \frac{t^2}{T_s^2} \quad (14)$$

Then it can be shown that

$$\frac{\delta I1}{\delta I} = \frac{m2 - m_x - m_y(D+D1)}{m1 + m_x + m_y(D+D1)} \quad (15)$$

Here  $m2$  and  $m1$  are the turn on and turn off slopes of the inductor current under steady state. If the right hand side of (15) is  $<1$  or equation (16) is satisfied then state stability under this type of current mode control is ensured .

$$m_x + m_y(D + D1) > \frac{m2 - m1}{2} \quad (16)$$

For small perturbation we may assume that  $D \approx D1$ . Then for Boost rectifier with PSM the condition for steady state stability can be expressed as (17)

$$\frac{V_o}{R_e T_s} - \frac{V_o}{L} + \frac{2DV_o}{L} > \frac{DV_o}{2L} - \frac{(1-D)V_o}{2L} \quad (17)$$

which can be simplified as

$$\frac{2L}{R_e T_s} > (1 - 2D) \quad (18)$$

where

$$\frac{1}{R_e} = \frac{2}{RM_g^2} - \frac{T_s}{2L} (1 - M_g \frac{8}{3\pi}) \quad (19)$$

and

$$M_g = \frac{v_{g,\max}}{V_o} \quad (20)$$

$R$  is the load resistance and  $D$  is the duty ratio.

In CCM, the minimum duty ratio  $D_{\min}$  can be expressed as (21). Defining  $K$  as in (22), it can be concluded that steady state stability condition for PSM controlled Boost rectifier is guaranteed if (23) is satisfied.

$$D_{\min} = 1 - M_g \quad (21)$$

$$K = \frac{2L}{RT_s} \quad (22)$$

$$K > \frac{M_g^3(1.151)}{2} \quad (23)$$

The right hand side of (23) can be defined as the critical  $K$  for stability under PSM.

$$K_{STAB} = \frac{M_g^3}{2}(1.151) \quad (24)$$

#### IV. DCM OPERATION

In the DCM, the inductor current is zero at the beginning of a switching period. Therefore the duty ratio will be decided by (25)

$$\frac{v_g dT_s}{L} = I_{ref}(1-d) + \frac{V_o T_s}{L} d(1-d) \quad (25)$$

But under DCM

$$v_g < (1-d)V_o \quad (26)$$

Combining (25) and (26) we get the condition (27) for DCM,

$$I_{ref} < 0 \quad (27)$$

When  $I_{ref} = 0$  the inductor current has only ripple component as the current is zero at the beginning and end of each switching period. Under this condition the power balance equation can be written as (28)

$$\frac{V_o^2}{R} = \frac{2}{T} \int_0^{\frac{T}{2}} p(t) dt = \frac{2}{T} \int_0^{\frac{T}{2}} v_g \cdot i_{gav} dt \quad (28)$$

Here  $T$  is the period of the line voltage waveform.

Now  $i_g$  can be replaced by (29) and using definitions of  $K$  and  $M_g$  (30) can be expressed as

$$i_{gav} = \frac{v_g dT_s}{2L} \quad (29)$$

$$\frac{V_o^2}{R} = \frac{T_s v_{gm}^2}{2L} - \frac{T_s v_{gm}^2 M_g}{2L} \int_0^{\frac{T}{2}} \sin^3(2\pi/T) dt \quad (30)$$

From (30) the criteria for CCM can be obtained as

$$K > \frac{M_g^2}{2} \left(1 - M_g \frac{8}{3\pi}\right) \quad (31)$$

The right hand side of (31) can be defined as critical  $K$  for CCM of the PSM

$$K_{CCM\_PSM} = \frac{M_g^2}{2} \left(1 - M_g \frac{8}{3\pi}\right) \quad (32)$$

It has been shown in [2] that for CCM operation over the entire line half cycle the NLC critical  $K$  has to be defined as

$$K_{CCM\_NLC} = \frac{M_g^2}{2} \quad (33)$$

Fig. 6 shows plots of the two critical  $K$  s as function of  $M_g$ . It is clear from this figure as well as from equations (32) and (33) that over the entire range of  $M_g$

$$K_{CCM\_PSM} < K_{CCM\_NLC} \quad (34)$$

However it is not possible to take full advantage of the wider range of CCM operation for PSM as steady state stability problems are encountered. The stability problem is less severe at lower  $M_g$  as can be seen from Fig.6. This is because of the nonlinear compensating ramp that contributes very high negative slope at higher duty ratio.

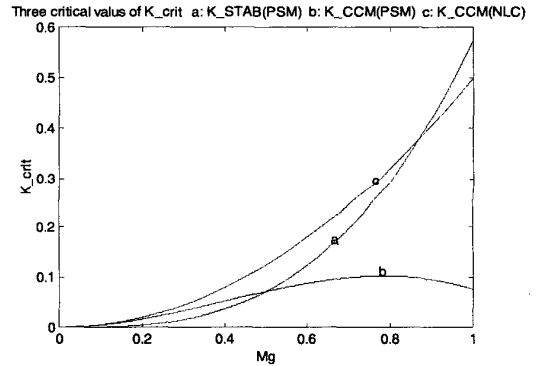


Fig. 6. For steady state stability  $K=(2L/RT_s) > K_{STAB}$  : (a)  
For CCM operation with PSM  $K > K_{CCM(PSM)}$  : (b)  
For CCM operation with NLC  $K > K_{CCM(NLC)}$  : (c)

A simulation waveform of inductor current ( $i_g$ ) verifying CCM of operation over the entire line half cycle is shown in Fig. 7. The following table gives the parameter values that are used in the simulation.

TABLE I

$V_g(rms)$	110V
$M_g$	0.7

$L$	$2.5mH$
$F_s$	$50KHz$
$K$	$0.2$
$C$	$47\mu F$

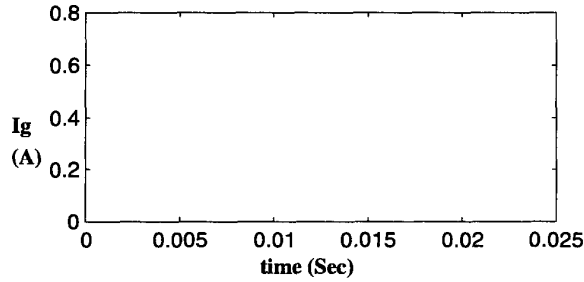


Fig. 7. Simulation waveform of inductor current  $I_g$  showing CCM operation for the entire line half cycle.  $M_g=0.7$   $K=0.2$

### V. LOW FREQUENCY SMALL SIGNAL MODEL

The state space averaged model of the Boost converter power stage is well known [5]. We need to determine the linear small signal low frequency model of the modulator that has been proposed here. These two models can then be combined to obtain the complete model of Boost rectifier controlled by PSM. For simplicity the procedure described in [3] is followed here to perturb the inductor current under steady state and get a modulator model. However the unified modulator model of [6] which perturbs two simultaneous equations under steady state can also be used. The modulator dynamics can be incorporated into the small signal ( $\hat{\cdot}$ ) averaged state space description of the Boost Converter by replacing  $\hat{d}$  with  $\hat{i}_{ref}$ . The perturbation of (35) results in (36).

$$i_l + \frac{v_g d T_s}{2L} = i_{ref} - i_{ref} d + \frac{v_o d T_s}{L} - \frac{v_o d^2 T_s}{L} \quad (35)$$

$i_l$  is the average current in the inductor during  $T_s$ .

$$\left[ \frac{V_g T_s}{2L} + \frac{2DV_o T_s}{L} + I_{ref} - \frac{V_o T_s}{L} \right] \hat{d} = (1-D)\hat{i}_{ref} - \hat{i}_l - \frac{DT_s \hat{v}_g}{2L} + \frac{D(1-D)T_s \hat{v}_o}{L} \quad (36)$$

The basic objective of this exercise is to determine the loop gain transfer function  $G_V(s)$  as shown in Fig.8.

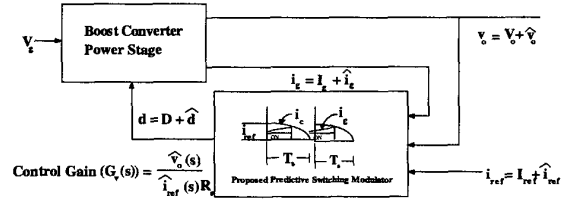


Fig. 8. Derivation of small signal control gain transfer function  $G_V(s)$  of PSM controlled Boost rectifier

### VI. EXPERIMENTAL RESULTS

A 200W Boost rectifier is built to experimentally verify PSM. The output voltage is regulated at 350V dc. Fig. 9 shows the circuit that generates the carrier waveform of PSM.

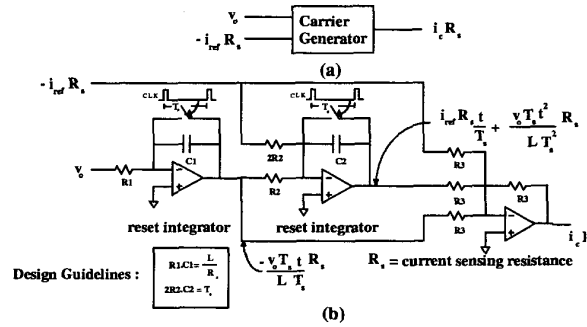


Fig. 9. (a) Carrier Generator Block of PSM  
(b) Circuit realization of PSM Carrier Generator

The selection of the circuit components should be governed by the following equations.

$$R_1 C_1 = \frac{L}{R_s} \quad (37)$$

$$2R_2 C_2 = T_s \quad (38)$$

$R_s$  is the equivalent current sensing resistance and  $L$  is the inductance of the Boost rectifier. The experimental waveforms of the line voltage, line current, inductor current and the carrier waveform are shown in Fig.10.

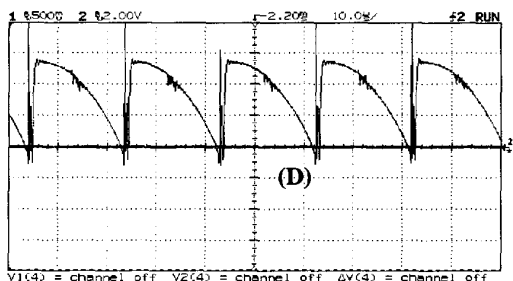
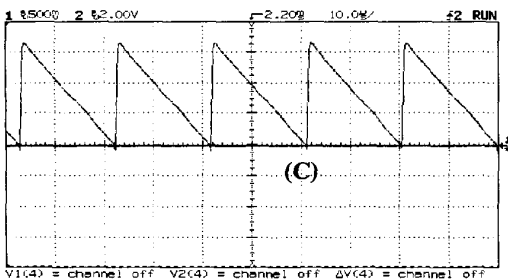
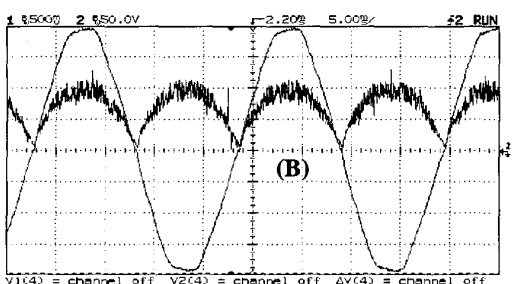
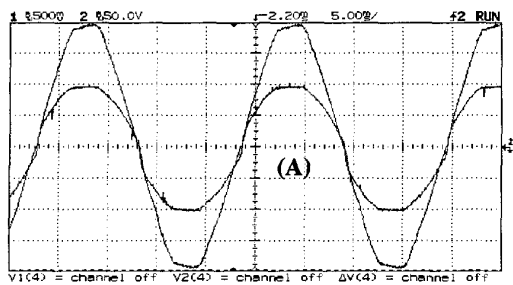


**Fig. 10 Experimental Results of PSM Controlled Rectifier:**

- (A)  $V_{in}$  and  $I_{in}$
- (B)  $V_{in}$  and  $I_g$
- (C) Carrier of PSM at  $V_o$  regulated at 0V
- (D) Carrier of PSM when  $V_o$  is 350V.

## VII. CONCLUSION

In this paper a predictive switching modulator (PSM) for high power factor operation of Boost rectifier is proposed. The modulator implements the switching function in such a way that the actual current lies on the top of a reference current profile that has the same shape as the line voltage waveform. This is achieved without input voltage sensing and multiplier circuitry in the control loop. The advantage of PSM lies in the extended CCM of operation of the converter. It is based on instantaneous switch current sensing and generation of a carrier that has second order compensating component. The steady state stability analysis of the modulator is carried out. A procedure for the development of small signal low frequency model of the modulator is brought out. Experimental results of the prototype unit show high power factor of 0.99 and 3.6% THD in the line current when THD of the line voltage is 2.4%.

## REFERENCES

- [1] J.P.Gegner and C.Q.lee, "Linear peak current mode control: A simple active power factor correction control technique for continuous conduction mode," in PESC'96, June 1996, pp. 196-202.
- [2] D.Maksimovic, Y.Jang, and R.Erickson, "Nonlinear-carrier control for high power factor boost rectifiers," in APEC'95, pp.635-641.
- [3] S. Hsu, A. Brown, L. Rensink and R.D. Middlebrook, "Modelling and analysis of switching dc-to-dc converters in constant-frequency current-programmed mode," in PESC'79, June 18-22, 1979
- [4] R.Zane and D. Maksimovic', "Nonlinear-carrier control for high-power-factor rectifiers based on up-down switching converters," in IEEE Transactions on Power Electronics, vol.13, pp .213-221, 1998
- [5] R.D.Middlebrook and S.M. C'uk, "A general unified approach to modelling switching converter power stages" in IEEE PESC record, pp 18-34, 1976
- [6] F. Dong Tan and R.D.Middlebrook, "A unified model for current-programmed converters," in IEEE Transactions on Power Electronics, vol.10, no.4, pp. 397-408, July 1995